

Table V. Valence Force Field for $\text{Fe}(\text{CO}_2)(\text{PMe}_3)_4^a$

vibrational modes	init values	final values
$\nu(\text{FeP})$	1.6	$\nu(\text{FeP}_{\text{ax}}) = 1.42$ $\nu(\text{FeP}_3) = 1.9$ $\nu(\text{FeP}_4) = 1.5$
$\nu(\text{FeO})$	0.9	0.9
$\nu(\text{FeC})$	0.9	1.18
$\nu_s(\text{PC}_3)$	2.75	2.55
ν_a - and ν_s' (PC_3)	2.42	2.22
$\nu(\text{C-O})$	5.3	6.33
$\nu(\text{C=O})$	9.6	8.7
δ'_s - and δ_a (PC_3)	0.64	<i>b</i>
$\delta(\text{CFeO})$	0.25	<i>b</i>
$\delta(\text{COFe})$	0.35	<i>b</i>
$\delta(\text{OCFe})$	0.35	<i>b</i>
$\delta(\text{C=O})$	1.09	0.79
$\delta(\text{PFeP})$	0.34	<i>b</i>
$\delta(\text{PFeO})$	0.44	0.30
$\delta(\text{PFeC})$	0.28	<i>b</i>
$\gamma(\text{C=O})$	0.68	0.74
$r_{\parallel}(\text{PC}_3)$	0.46	<i>b</i>
$r_{\perp}(\text{PC}_3)$	0.46	<i>b</i>
$\delta_s(\text{PC}_3)$	0.46	0.57
$\tau(\text{FeP})$	0.0005	0
$\tau(\text{FeO})$	0.0005	0
$\tau(\text{FeC})$	0.0005	0
$\tau(\text{PP})$	0	<i>b</i>
$f[\nu(\text{C-O}), \delta(\text{C=O})]$	-0.4	0.13
$f[\nu(\text{FeP}), \nu(\text{FeP}_{\text{opp}})]$	0.12	0.33
$f[\nu(\text{FeP}), \delta_s(\text{PC}_3)]$	-0.09	-0.15
$f[\delta(\text{C=O}), \nu(\text{C=O})]$	0.65	0.32
$f[\nu(\text{C-O}), \nu(\text{C=O})]$	0	0.6
$f[\nu(\text{FeC}), \delta(\text{C=O})]$	-0.2	-0.4
$f[\delta(\text{OCFe}), \delta(\text{C=O})]$	0	0.2
$f[\nu(\text{FeO}), \delta(\text{C=O})]$	0	<i>b</i>
$f[\delta(\text{C=O}), \nu_s(\text{PC}_3)]$	0	0.45
$f[\delta(\text{C=O}), \nu(\text{FeP})]$	0	<i>b</i>
$f[\delta(\text{COFe}), \delta(\text{C=O})]$	0	0.2

^a Force constants are given in $\text{mdyn}\cdot\text{\AA}^{-1}$ for bonds, $\text{mdyn}\cdot\text{\AA}\cdot\text{rad}^{-2}$ for angles, and $\text{mdyn}\cdot\text{rad}^{-1}$ for bond-angle interactions. ^b Final value equal to the initial one.

complexes. Therefore, the most important part of this paper is devoted to the spectroscopic characterization of the bonding mode of coordination CO_2 by means of FTIR spectroscopy and normal coordinate analysis.

If we compare the $f[\nu(\text{C=O})]$ and $f[\nu(\text{CO})]$ force constants in these complexes, it appears that the gap between both bonds, along with the value of the interaction force constant $f[\nu(\text{C=O}), \nu(\text{CO})]$, is indicative of the electronic delocalization on the CO_2 unit and then allows discrimination between true $\eta^2\text{-C,O}$ and $\eta^1\text{-C}$ coordinations. Carbon dioxide has been found to be side-on coordinated in $\text{trans-Mo}(\text{CO}_2)_2(\text{PMe}_3)_4$ whereas the bonding is intermediate between $\eta^2\text{-C,O}$ and $\eta^1\text{-C}$ in $\text{Fe}(\text{CO}_2)(\text{PMe}_3)_4$.

It then appears that results obtained by matrix isolation IRTF spectroscopy¹⁴ can be applied to organometallic complexes. But coligands play an important role, as they can modify the spectra when coupling occurs in the molecule by structural effects. Indeed, in the molybdenum complex where the CO_2 lies in a plane perpendicular to other phosphine ligands, no coupling occurs and the CO_2 units present pure vibrational modes. On the contrary, the simultaneous presence of CO_2 and PMe_3 in the equatorial plane of the iron compound leads to a large modification of the $\delta(\text{C=O})$ mode and the expected isotopic shifts. Only normal coordinate analysis has allowed the exact assignment of all the mixed vibrational modes in this complex.

We have also shown that the existence of a mode in the 500–630- cm^{-1} region, with a large ^{13}C isotopic effect (around 20 cm^{-1}), is characteristic of a side-on or C coordination. This mode is easy to characterize because no close frequency appears in the same area and it belongs to a special symmetry class (out-of-the-plane motions) so that it is always pure.

Finally, such descriptions have to be related with the ability of such bonds to give important dynamic effects, which modulate the vibrational motion of the CO_2 ligand.

This paper has been largely devoted to the characterization of the CO_2 bonding mode to the metal in $\text{trans-Mo}(\text{CO}_2)_2(\text{PMe}_3)_4$ and $\text{Fe}(\text{CO}_2)(\text{PMe}_3)_4$ and has revealed the important role played by the analysis of isotopic labeling and normal coordinate treatment for this purpose. In the second part, we shall present the study of the CO_2 bonding mode in $\text{Cp}_2\text{Ti}(\text{CO}_2)(\text{PMe}_3)$.

Acknowledgment. We thank Prof. E. Carmona for the gift of a sample of $\text{trans-Mo}(\text{CO}_2)_2(\text{PMe}_3)_4$ and for permission to quote his unpublished IR data on molybdenum compounds. We thank J. C. Cornut for his technical assistance and the many people who have discussed these results with us, particularly Profs. M. Aresta and D. Astruc and Dr. M. Tranquille for critical reading of the manuscript.

Contribution from the Laboratoire de Spectroscopie Moléculaire et Cristalline, URA 124, CNRS, Université de Bordeaux I, 351 Cours de la Libération, 33405 Talence Cedex, France

Carbon Dioxide Coordination Chemistry. 2.¹ Synthesis and FTIR Study of $\text{Cp}_2\text{Ti}(\text{CO}_2)(\text{PMe}_3)$

Corine Jegat, Monique Fouassier, Michel Tranquille, and Joëlle Mascetti*

Received July 27, 1990

Synthesis and thermal evolution of $\text{Cp}_2\text{Ti}(\text{CO}_2)(\text{PMe}_3)$ have been revisited. The FTIR spectra in the solid state and in solution in various solvents of the complex and of its isotopic labeled derivatives ($^{13}\text{CO}_2$, C^{18}O_2) have been investigated. Normal coordinate analysis was performed with different structural hypotheses and led to the conclusion that FTIR spectra indicate that CO_2 is C-coordinated to the titanium in this complex. Complete assignments of FTIR spectra and the valence force field are then proposed. The results of this paper are combined with those of part 1 (preceding paper) to propose an overall scheme for the infrared spectroscopic characterization of CO_2 complexes.

Introduction

This is the second of two papers investigating the infrared characterization of CO_2 complexes. The first one¹ was concerned with the study of $\text{trans-Mo}(\text{CO}_2)_2(\text{PMe}_3)_4$ and $\text{Fe}(\text{CO}_2)(\text{PMe}_3)_4$, and we found evidence for a side-on CO_2 -metal bonding mode

in the molybdenum complex whereas the bonding is intermediate between an $\eta^1\text{-C}$ and a side-on arrangement in the iron compound.

This paper is devoted largely to the study of $\text{Cp}_2\text{Ti}(\text{CO}_2)(\text{PMe}_3)$ and focuses, in particular, on the importance of two vibrational modes that are highly sensitive to the CO_2 bonding scheme in the

* To whom correspondence should be addressed.

(1) Part 1: Jegat, C.; Fouassier, M.; Mascetti, J. *Inorg. Chem.*, preceding paper in this issue.

complex: the symmetric stretching $\nu(\text{CO})$ and the out-of-the-plane bending $\gamma(\text{C}=\text{O})$ modes.

Our strategy, therefore, has been to use isotopic labeling (^{13}C , ^{18}O) to assign infrared spectra and to transfer previous valence force fields to fit the best geometry for $\text{Cp}_2\text{Ti}(\text{CO})_2(\text{PMe}_3)$.

Experimental Section

Chemicals. Solvents were purchased from commercial sources (SDS), distilled, and bubbled with argon before use. Air-sensitive compounds and solutions were handled under argon with the use of Schlenk equipment in conjunction with a vacuum-argon manifold and glovebox.

PMe_3 and Cp_2TiCl_2 were obtained respectively from Strem Chemicals and Aldrich and used without further purification.

FTIR Spectra. FTIR spectra were recorded for Nujol mulls under argon, using a Bruker 113V Fourier transform interferometer (4000–200 cm^{-1}) or a Nicolet 740 Fourier transform interferometer (4000–400 cm^{-1}) with CsI windows and a Nicolet 20F Fourier transform interferometer (700–100 cm^{-1}) with polyethylene windows; the resolution being 2 cm^{-1} in all cases.

It is important to note that on the contrary to the previously studied compounds $\text{Mo}(\text{CO})_2(\text{PMe}_3)_4$ and $\text{Fe}(\text{CO})_2(\text{PMe}_3)_4$,¹ the FTIR spectra of $\text{Cp}_2\text{Ti}(\text{CO})_2(\text{PMe}_3)$ and its labeled derivatives did not allow us to fully exploit the region below 400 cm^{-1} , despite several attempts on various spectrometers and samples.

Solutions were handled by means of a variable temperature and path liquid cell, described in the previous paper.¹ Experiments were also achieved by means of a variable path liquid cell SPECAC with CsI windows and of a "Specacflow ATR" cell equipped with a ZnSe crystal. Temperature-controlled (especially low) solution-phase samples under gaseous atmospheres (especially inert) are to be studied to fully understand vibrational spectra of CO_2 complexes, as explained in previous paper.¹ So, referring to D. J. Darensbourg and colleagues' work,² we used ATR technique to run FTIR spectra in solution, as path length adjustments (below 50 μm) are often a problem with conventional transmission cells used at low temperature (below 0 $^\circ\text{C}$) especially with polar solvents (THF, chloroform) having strong absorptions. Solutions were pumped from a Schlenk flask through the ATR cell and back into the flask by means of a peristaltic pump with polyethylene tubing, except for the short portion in the pump, which was made of silicone tubing. This tubing was not chemically resistant to some solvents (especially THF) for long times but was sufficient for a few hours and allowed the scanning of FTIR spectra, which need only a few minutes. The advantage of this apparatus was that it allowed the use of quite small volumes of solution (about 8 mL are sufficient to fill the apparatus without bubbles). The flask is cooled in a constant-temperature bath filled with ethanol at $-50\text{ }^\circ\text{C}$; the solution is then maintained at $-30\text{ }^\circ\text{C}$. The atmosphere inside the optical bench is kept dry by means of a dry air purge to prevent condensation on the crystal. The use of a Schlenk flask allows the maintenance of an inert atmosphere in the all tubing and cell by circulation of argon.

Despite several attempts, it was impossible to obtain Raman spectra of this pale yellow complex. No diffusion signal was obtained by using red and yellow exciting lines, and strong fluorescence appeared under exposure to green and blue laser lines, hindering any Raman diffusion spectrum detection.

Synthesis of $\text{Cp}_2\text{Ti}(\text{CO})_2(\text{PMe}_3)$. As our attempts to reproduce the synthesis of $\text{Cp}_2\text{Ti}(\text{PMe}_3)_2$ by published methods³ were unsuccessful, we propose the following procedure. A mixture of Cp_2TiCl_2 (0.5 g), Hg/Na amalgam (48 g, 1% Na), PMe_3 (1 mL), and THF (20 mL) was stirred at room temperature. The red suspension turned rapidly green and then blue, becoming brown after 1 h. After 12 h, the solution was filtered, the solvent removed in vacuo, and the residue extracted with pentane. Black crystals of $\text{Cp}_2\text{Ti}(\text{PMe}_3)_2$ were obtained (0.2 g, yield 30%) after 12 h at 0 $^\circ\text{C}$ from concentrated solutions.

$\text{Cp}_2\text{Ti}(\text{PMe}_3)_2$ (0.2 g) was dissolved in pentane (10 mL) in a flask, and the mixture was cooled at $-180\text{ }^\circ\text{C}$. After evacuation, dry CO_2 was admitted (2 atm). The flask was allowed to warm at room temperature, and the solution was stirred for 10 min. An abundant yellow precipitate was formed, which was filtered off, washed with pentane, and dried in vacuo (yield 90%). $\text{Cp}_2\text{Ti}(\text{CO})_2(\text{PMe}_3)$ is best kept at 0 $^\circ\text{C}$ in the dark, under a CO_2 atmosphere.

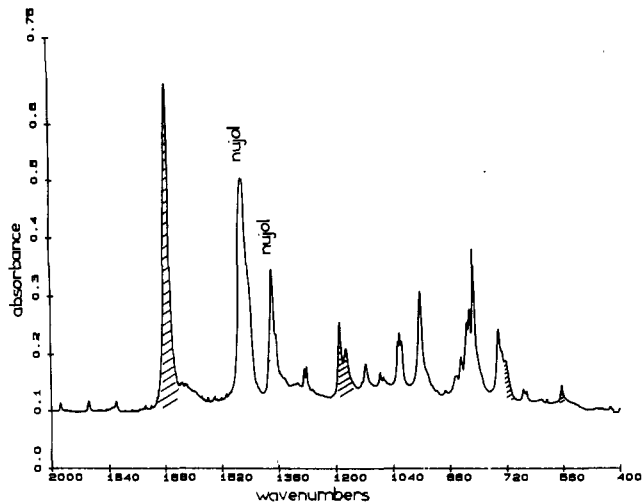


Figure 1. FTIR spectrum of solid $\text{Cp}_2\text{Ti}(\text{CO})_2(\text{PMe}_3)$ in a Nujol mull. (The hatching represents CO_2 absorptions.)

Slow thermal decomposition at room temperature under argon atmosphere principally gives the dicarbonyl $\text{Cp}_2\text{Ti}(\text{CO})_2$.

Solutions of $\text{Cp}_2\text{Ti}(\text{CO})_2(\text{PMe}_3)$ must be handled at $-20\text{ }^\circ\text{C}$. Thermal decomposition has not been fully elucidated, but CO_2 is no longer coordinated and infrared spectra reveal the presence of trimethylphosphine oxide.

Results and Discussion

General Strategy. As described in part 1, we will discuss the assignment of the observed infrared absorptions to fundamentals of each ligand (Cp, PMe_3 , CO_2) and the qualitative structural information directly accessible from the different isotopic data. Then we will show that enough vibrations are observed to lead to a normal coordinate analysis for the vibrations of either form, and we will discuss more quantitatively some structural parameters that are thereby possible to estimate.

At the molecular cluster scale, the complexation and activation of CO_2 on transition-metal centers has been studied in matrices⁴ and provided spectral reference points for comparison with organometallic species as well-defined, simple coordination compounds of CO_2 .

The previous study of molybdenum and iron complexes¹ gave us initial valence force fields that can be transferred for side-on complexes.

Supposing a given symmetry, it is possible to calculate from the experimental frequencies and isotopic shifts a complete harmonic force field for the fundamentals of this molecule, using the well-known Wilson's method.⁵ In absence of ab initio study on this system, one must assume a realistic geometry. This will be drawn from the X-ray structure obtained for $\text{Cp}_2\text{Ti}(\text{CO})(\text{PMe}_3)$.⁶

FTIR Study. (1) Solid-State Spectra. The FTIR spectrum of solid $\text{Cp}_2\text{Ti}(\text{CO})_2(\text{PMe}_3)$ in suspension in Nujol is given on Figure 1. We shall distinguish three parts in this spectrum, relative to each ligand: trimethylphosphine, cyclopentadienyl, and carbon dioxide.

PMe_3 . As for previously studied compounds,¹ we do not see important change in the spectra of free and coordinated PMe_3 . Concerning the region of importance (2000–400 cm^{-1}), bending modes of CH_3 are located at 1285 and 1279 cm^{-1} and one of the rocking modes is seen at 961 cm^{-1} whereas the other one, expected around 850 cm^{-1} , is obscured by strong absorptions due to the cyclopentadienyl group. The stretching ν_s - and $\nu'_s(\text{PC}_3)$ give, together with the CO_2 deformation mode (see previous paper¹), the congested set of bands around 730 cm^{-1} . The symmetric stretching $\nu_s(\text{PC}_3)$ is observed at 668 cm^{-1} , but we can note that

(2) Darensbourg, D. J.; Gibson, G. In *Experimental Organometallic Chemistry: a Practicum in Synthesis and Characterization*; ACS Symposium Series 357; American Chemical Society: Washington, DC, 1987; p 230.

(3) (a) Kool, L. B.; Rausch, M. D.; Alt, H. G.; Herberhold, M.; Thewalt, U.; Wolf, B. *Angew. Chem., Int. Ed. Engl.* **1985**, *24* (5), 400. (b) Kool, L. B.; Rausch, M. D.; Alt, H. G.; Herberhold, M.; Honold, B.; Thewalt, U. *J. Organomet. Chem.* **1987**, *320*, 37. (c) Alt, H. G.; Schwind, K. H.; Rausch, M. D. *J. Organomet. Chem.* **1987**, *321*, C9.

(4) Mascetti, J.; Tranquille, M. *J. Phys. Chem.* **1988**, *92*, 2177–2184.

(5) Wilson, E. B., Jr.; Decius, J. C.; Cross, P. In *Molecular Vibrations*; McGraw-Hill: New York, 1955.

(6) Kool, L. B.; Rausch, M. D.; Alt, H. G.; Herberhold, M.; Wolf, B.; Thewalt, U. *J. Organomet. Chem.* **1985**, *297*, 159.

Table I. Cyclopentadienyl Absorptions in Various Bis(cyclopentadienyl)titanium Compounds

$\text{Cp}_2\text{Ti}^{\text{IV}}\text{Cl}_2^a$	$\text{Cp}_2\text{Ti}^{\text{III}}\text{Cl}(\text{PMe}_3)^b$	$\text{Cp}_2\text{Ti}^{\text{III}}(\text{PMe}_3)_2^b$	$\text{Cp}_2\text{Ti}^{\text{II}}(\text{CO})_2^c$	$\text{Cp}_2\text{Ti}^{\text{II}}(\text{CO})_2(\text{PMe}_3)^b$	assgmt
1300 (vw)		1300 (m)	1423 (m)	1285 (m)	
	1260 (m)	1275 (m)	1263 (w)	1279 (m)	$\delta(\text{CH}_3)$
	1240 (m)				
	1230 (m)				
	1215 (m)				
1170 (w)		1170 (w)		1169 (m)	$\delta(\text{CH})$
1150 (w)	1150 (w)	1155 (w)			
1130 (w)	1130 (w)				
		1110 (m)	1110 (w)	1116 (m)	
	1100 (w)			1075 (w)	
1075 (vw)		1065 (w)	1060 (s)	1070 (w)	$\delta(\text{CCC})$
			1050 (m)	1062 (w)	
1025 (sh)	1020 (s)			1025 (m)	
		1015 (m)	1015 (s)	1019 (m)	$\delta(\text{CH})$
1012 (m)	1010 (s)	995 (m)	1000 (s)	1012 (m)	
995 (vw)		945 (s)			
955 (vw)	955 (s)	935 (s)		961 (m)	$r(\text{CH}_3)$
925 (vw)		920 (sh)			
		890 (w)	892 (w)		
865 (m)	860 (sh)	850 (sh)		860 (sh)	$\gamma(\text{CH})$
	850 (sh)	840 (sh)	840 (s)	846 (sh)	
		825 (sh)	830 (s)	830 (sh)	$r(\text{CH}_3)$
				822 (sh)	
			810 (s)		
818 (s)	805 (s)	790 (vs)	795 (vs)	811 (vs)	$\gamma(\text{CH})$
				800 (sh)	
				741 (m)	$\nu'_s(\text{PC}_3)$
	730 (s)	730 (m)	725 (w)	731 (m)	$\nu_s(\text{PC}_3)$
		700 (m)			
		685 (w)			
	675 (w)	665 (w)	665 (w)	672 (sh)	$\nu_s(\text{PC}_3)$
		645 (m)	615 (w)	668 (w)	
			555 (m)		
			490 (m)		$\nu(\text{TiC}), \delta(\text{MCO})$
			462 (s)		
	460 (vw)	460 (vw)		465 (vw)	
413 (sh)				427 (vw)	$\nu_s(\text{TiCp})$
400 (m)	400 (m)		405 (m)		$\nu(\text{TiCl}), \delta(\text{MCO})$
	380 (sh)	385 (m)		393 (w)	$\nu(\text{TiP})$
360 (m)	360 (w)				$\nu_s(\text{TiCp})$
		335 (w)			
300 (m)	290 (m)	285 (vw)			tilt(Cp_2Ti)
245 (m)	250 (m)				tilt(Cp_2Ti)

^a From ref 7. ^b From our work. ^c From ref 8.

a shoulder is present at 672 cm^{-1} . This will be discussed further.

Cp. We have used the assignments obtained for Cp_2TiCl_2 ⁷ to identify the absorptions due to the Cp ligands. We know, from previous NMR studies by Raush and colleagues⁶ that the electronic density on the Cp depends on the metal oxidation state. On infrared spectra, going from titanium(IV) to titanium(II), the most sensitive vibration to the metal oxidation state will be the out-of-the-plane bending $\gamma(\text{CH})$ mode. For example, $\gamma(\text{CH})$ is found to be at 818 cm^{-1} in $\text{Cp}_2\text{Ti}^{\text{IV}}\text{Cl}_2$,⁷ whereas it is located at 795 cm^{-1} in $\text{Cp}_2\text{Ti}^{\text{II}}(\text{CO})_2$, leading to a frequency shift of 23 cm^{-1} . Table I lists the wavenumbers assigned to Cp ligands in various bis(cyclopentadienyl) compounds: $\text{Cp}_2\text{Ti}^{\text{IV}}\text{Cl}_2$ as starting material, $\text{Cp}_2\text{Ti}^{\text{III}}\text{Cl}(\text{PMe}_3)$ as isolated intermediate in the synthesis of $\text{Cp}_2\text{Ti}(\text{PMe}_3)_2$, and $\text{Cp}_2\text{Ti}^{\text{III}}(\text{PMe}_3)_2$, $\text{Cp}_2\text{Ti}^{\text{III}}(\text{CO})_2(\text{PMe}_3)$, and $\text{Cp}_2\text{Ti}^{\text{II}}(\text{CO})_2$ ⁸ for comparison. Most important vibrations for understanding the vibrational spectrum of the $\text{Cp}_2\text{Ti}(\text{CO})_2(\text{PMe}_3)$ compound are located in the region 1300–200 cm^{-1} .

The band at 1170 cm^{-1} can be assigned to $\delta(\text{CH})$, but the intensity is much more important in $\text{Cp}_2\text{Ti}(\text{CO})_2(\text{PMe}_3)$ than in other Cp_2TiL_2 compounds. This problem will be discussed in the

next section. At 1125 (sh) and 1115 cm^{-1} (m) are expected $\nu(\text{CC})$ and $\delta_s(\text{CH})$, but the latter one will be discussed further (see next section). At 1074 (w) and 1066 cm^{-1} (w), we find the bending modes $\delta(\text{CCC})$ of the Cp cycles. Then a triplet of medium intensity located at 1025, 1020, and 1013 cm^{-1} is assigned to other bending modes $\delta(\text{CH})$. At 860 (sh) and 811 cm^{-1} (vs) we find the out-of-the-plane bending modes $\gamma(\text{CH})$.

As already underlined in the Experimental Section, the infrared spectrum below 500 cm^{-1} is very poor, with only three weak bands, and there is no signal below 300 cm^{-1} that would be assigned to the tilt motions of the Cp_2Ti moiety that are however of medium intensity in Cp_2TiCl_2 at 300 and 245 cm^{-1} .

CO₂. As in part 1,¹ assignments will be made with the help of isotopic shifts observed on infrared spectra of labeled compounds $\text{Cp}_2\text{Ti}^{13}\text{CO}_2(\text{PMe}_3)$ and $\text{Cp}_2\text{Ti}(\text{C}^{18}\text{O}_2)(\text{PMe}_3)$. At 1671 cm^{-1} , we find an absorption that is shifted to 1629 cm^{-1} by ¹³C labeling and to 1648 cm^{-1} by ¹⁸O enrichment. This band is assigned to a C=O stretching mode. Furthermore, the infrared spectrum of a compound made with an equimolar mixture of ¹²CO₂/¹³CO₂ exhibits a doublet pattern at 1671 and 1629 cm^{-1} , as expected for a compound containing only one CO₂ moiety per molecule.

In the region where are located the CO stretching modes (1200–1000 cm^{-1}), we observe three bands at 1187 (ms), 1169 (m) and 1115 cm^{-1} (mw) (Figure 2). In the ¹³C-labeled compound, only two bands of equal intensity are observed at 1167 (m) and 1155 cm^{-1} (m), whereas, in the ¹⁸O-enriched complex, the three bands are present but with dramatic changes in intensity:

- (7) (a) Malowski, E., Jr.; Nakamoto, K. *Applied Spectrosc.* **1971**, *25*, 187.
 (b) Samuel, E.; Ferrer, R.; Bigorgne, M. *Inorg. Chem.* **1973**, *12*, 881.
 (c) Balducci, C.; Bencivenni, L.; De Rosa, G.; Gigli, R.; Martini, B.; Nunziante-Cesaro, S. *J. Mol. Struct.* **1980**, *64*, 163.
 (8) Calderazzo, F.; Salzmann, J. J.; Mosimann, P. *Inorg. Chim. Acta* **1967**, *1*, 65.

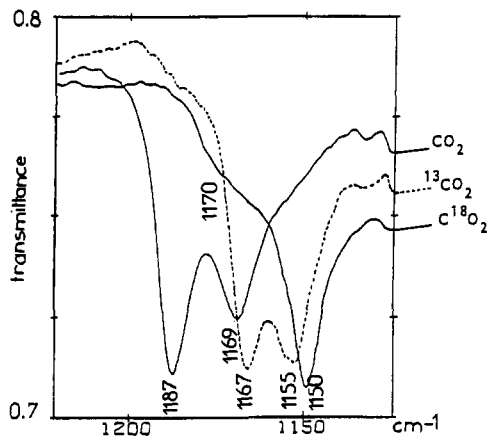


Figure 2. Detailed part of the infrared spectrum of solid $\text{Cp}_2\text{Ti}(\text{CO}_2)(\text{PMe}_3)$ and its labeled derivatives (^{13}C , ^{18}O) in the region $1130\text{--}1220\text{ cm}^{-1}$.

1170 (w, sh) , 1150 (ms) , and $1100\text{ cm}^{-1}\text{ (m)}$. Finally, the infrared spectrum of the mixed $^{12}\text{C}/^{13}\text{C}$ compound is found to be the sum of the ^{12}C and ^{13}C spectra, so that the conclusion is that the observed pattern is due to only one CO_2 moiety per molecule.

If we consider that the band located at 1115 cm^{-1} is probably due to an oxygenated impurity, the remaining doublet can rise from: (i) the presence of an impurity; (ii) a crystal effect; (iii) a Fermi resonance effect; (iv) a coupling between $\nu(\text{CO})$ and a motion of the Cp moiety located at a close frequency; (v) the existence of two conformers. The reproducibility of the spectrum scanned with samples originating from a different synthesis rules out the first hypothesis.

Concerning a Fermi resonance effect, we must consider a combination or an overtone level coming in close proximity to a fundamental belonging to the same symmetry class. It results in an intensity lending to the latter, and the degree of mixing between the two resulting levels (ν_+ , ν_-) will be a function of the closeness of the position of the two original levels (ν_a , ν_c). The position of the unperturbed levels can be deduced from the simple expressions⁹

$$\nu_a = \nu_- + (\nu_+ - \nu_-)/(R + 1) \quad \nu_c = \nu_+ - (\nu_+ - \nu_-)/(R + 1)$$

with the intensity ratio

$$R = I_-/I_+$$

The calculation of ν_a (fundamental level) and ν_c (combination or overtone) for each isotopic compound gives the following results: $\nu_a(^{12}\text{C}^{16}\text{O}_2) = 1180\text{ cm}^{-1}$ with $\nu_c = 1176\text{ cm}^{-1}$, $\nu_a(^{13}\text{C}^{16}\text{O}_2) = 1161\text{ cm}^{-1}$ with $\nu_c = 1160\text{ cm}^{-1}$, and $\nu_a(^{12}\text{C}^{18}\text{O}_2) = 1151\text{ cm}^{-1}$ with $\nu_c = 1165\text{ cm}^{-1}$. If we consider ν_c as an overtone, these results locate the fundamental level in the range $580\text{--}588\text{ cm}^{-1}$. If we consider ν_c as a combination, a lot of possibilities arise as the symmetry of the overall molecule is very low (C_1 or C_3). We must now assign the remaining part of the $\text{Ti}(\text{CO}_2)$ moiety motions to find an answer to this question.

In Figure 3 is drawn the spectral region $760\text{--}690\text{ cm}^{-1}$ for the three isotopic compounds. We can see that the absorption located at 722 cm^{-1} is shifted to 711 cm^{-1} by ^{13}C labeling and to 700 cm^{-1} by ^{18}O enrichment. This will be assigned to the OCO angle deformation $\delta(\text{C}=\text{O})$. This congested region shows two other absorptions at 741 and 731 cm^{-1} . The one located at 741 cm^{-1} exhibits small isotopic shifts by isotopic labeling (respectively 3 and 4 cm^{-1} by ^{13}C and ^{18}O enrichment). We thus assign it to the ν_s component of the PC_3 stretchings, which is located in the OCO plane. The other component $\nu_a(\text{PC}_3)$, which gives a resultant motion perpendicular to the OCO plane, shows no frequency shift and is located at 731 cm^{-1} . We thus observe a coupling between the $\delta(\text{C}=\text{O})$ and $\nu_s(\text{PC}_3)$ motions, as observed in the case of the $\text{Fe}(\text{CO}_2)(\text{PMe}_3)_4$ complex between $\delta(\text{C}=\text{O})$ and $\nu_s(\text{PC}_3)$ (see part 1).¹ We also must keep in mind the presence of Nujol absorptions

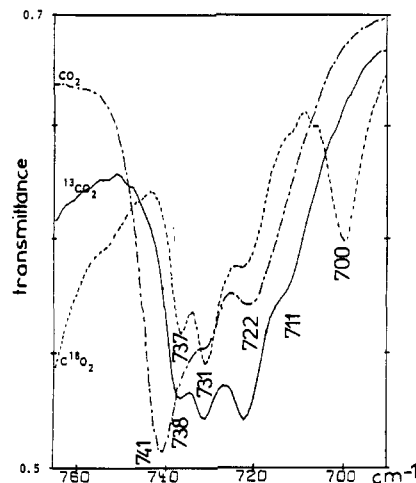


Figure 3. Detailed part of the infrared spectrum of solid $\text{Cp}_2\text{Ti}(\text{CO}_2)(\text{PMe}_3)$ and its labeled derivatives (^{13}C , ^{18}O) in the region $690\text{--}760\text{ cm}^{-1}$.

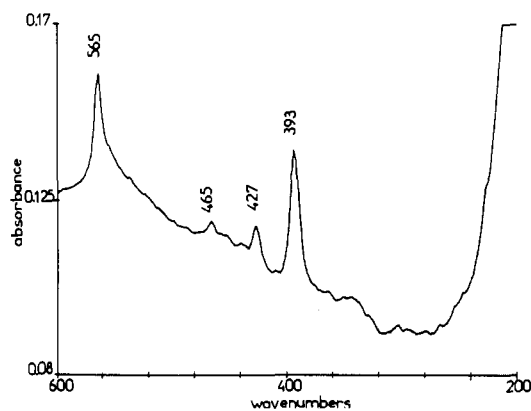


Figure 4. Far-infrared spectrum of solid $\text{Cp}_2\text{Ti}(\text{CO}_2)(\text{PMe}_3)$ in a Nujol mull.

in our spectra, which contribute to the congestion of this region with an absorption at 723 cm^{-1} . We can thus conclude that the $\delta(\text{C}=\text{O})$ motion gives only *one* absorption in this region. If we consider the coupling between the $\delta(\text{C}=\text{O})$ and $\nu_s(\text{PC}_3)$ motions, the total isotopic effects observed on these modes are 14 cm^{-1} by $^{12}\text{C}/^{13}\text{C}$ labeling and 26 cm^{-1} by $^{16}\text{O}/^{18}\text{O}$ enrichment.

The absorption located at 565 cm^{-1} is shifted from 18 cm^{-1} by ^{13}C labeling and 5 cm^{-1} with ^{18}O enrichment. So by analogy with previous results (see part 1),¹ we assign this band to the out-of-the-plane deformation of the $\text{C}=\text{O}$ vibrator, $\gamma(\text{C}=\text{O})$. So, coming back to the question of the existence of a Fermi resonance for $\nu(\text{CO})$, we can see that the $\gamma(\text{C}=\text{O})$ absorption is located at a too low frequency (565 cm^{-1} vs $580\text{--}588\text{ cm}^{-1}$ expected) to be at the origin of a Fermi resonance between its first overtone (1130 cm^{-1}) and $\nu(\text{CO})$ (fundamental expected at 1180 cm^{-1}). Furthermore, the $\gamma(\text{C}=\text{O})$ band for enriched ^{13}C compound is found at 547 cm^{-1} , which gives a first overtone at 1084 cm^{-1} , very far from the fundamental $\nu(\text{CO})$ level expected at 1161 cm^{-1} . So, if the doublet pattern observed for $\nu(\text{CO})$ is due to a Fermi resonance effect, it cannot be with the first overtone of $\gamma(\text{C}=\text{O})$.

Let us have a look now at the low-frequency region. As outlined in the Experimental Section, the far-IR spectrum exhibits very few absorptions, the strongest one being located at 393 cm^{-1} (see Figure 4). Two other very weak bands are seen at 465 and 427 cm^{-1} . None of them presents frequency shifts by labeling with ^{13}C or ^{18}O CO_2 isotopes. The attribution will then be made by comparison with Cp_2TiCl_2 ⁷ and other CO_2 complexes.¹ So the metal-phosphorous stretching is assigned to the band at 393 cm^{-1} and the one at 427 cm^{-1} is thought to be the out-of-phase titanium-cyclopentadienyl stretching $\nu_a(\text{TiCp})$ (found at 413 cm^{-1} in Cp_2TiCl_2).

Figure 5 shows the evolution of the FTIR spectrum when the complex is allowed to stay several weeks at room temperature in

(9) Fernandez-Bertran, J.; Ballester, L.; Dobrihalova, L.; Sanchez, N.; Arrieta, R. *Spectrochim. Acta* **1968**, *24A*, 1765.

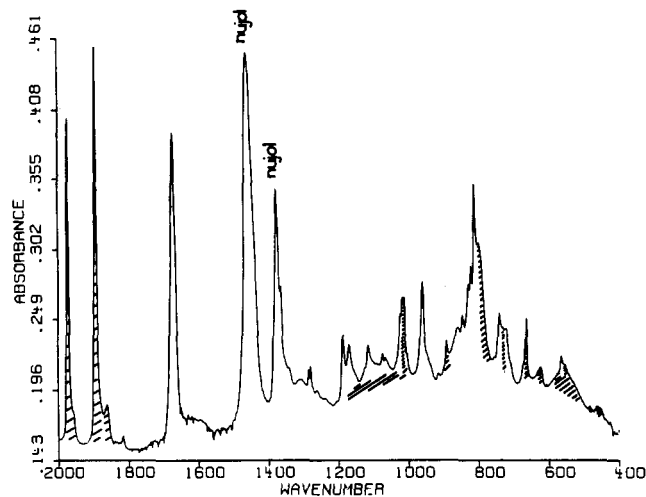


Figure 5. Evolution of the FTIR spectra of solid $\text{Cp}_2\text{Ti}(\text{CO}_2)(\text{PMe}_3)$ in a Nujol mull upon slow decomposition at room temperature under argon. (The hatching represents new features in the spectrum compared to that in Figure 1.)

the Nujol mull. New bands appear that can be assigned to the compound $\text{Cp}_2\text{Ti}(\text{CO})_2^8$ with main new absorptions at 1974 (vs) and 1894 cm^{-1} (vs) for $\nu(\text{C}\equiv\text{O})$, 1016 (m) for $\delta(\text{CH})$, 800 (s) for $\gamma(\text{CH})$, and 664 (ms), 622 (mw), 553 (mw), 490 (w), and 462 cm^{-1} (w) for $\delta(\text{TiCO})$ and $\nu(\text{TiC})$ vibrations.

Surprisingly, no signal indicating the presence of oxidized compounds of phosphine or titanium is detected, apart from a thickness of the region 1200–1050 and 600–500 cm^{-1} and bands of medium-weak intensities at 1000 (sh), 891, and 725 cm^{-1} (sh).

The presence of the monocarbonyl compound $\text{Cp}_2\text{Ti}(\text{CO})(\text{PMe}_3)^{10}$ is also detected with the absorption $\nu(\text{CO})$ at 1861 cm^{-1} .

So the mechanism of thermal decomposition screened from oxygen is not clear. This suggests the existence of binuclear bridged intermediates in the reaction. Anyway, the main conclusion is that, considering the 1200–1000- cm^{-1} region, the 1187 and 1169 cm^{-1} absorptions keep the same relative intensities, showing that they belong to the same entity.

So it appears now that study in solution is necessary to go further in the interpretation.

(2) Solution Spectra. In order to assign the doublet at 1187, 1169 cm^{-1} for solid $\text{Cp}_2\text{Ti}(\text{CO}_2)(\text{PMe}_3)$, we ran some spectra in solution at -20°C in chloroform and in dichloromethane. Figure 6 shows the results obtained. The doublet is no longer observed, and only one band is seen at 1184 cm^{-1} in CHCl_3 and at 1186 cm^{-1} in CH_2Cl_2 . It then becomes evident that the doublet pattern arises from an intermolecular coupling (so-called "crystal effect") and that the *maximum* values for isotopic frequency shifts of $\nu(\text{CO})$ stretching are then $1187 - 1155 = 32 \text{ cm}^{-1}$ by $^{12}\text{C}/^{13}\text{C}$ labeling and $1187 - 1150 = 37 \text{ cm}^{-1}$ by $^{16}\text{O}/^{18}\text{O}$ enrichment.

We can also note that the shoulder at 672 cm^{-1} of the $\nu_s(\text{PC}_3)$ absorption disappears in solution. Only a band at 667 cm^{-1} remains, showing that this feature also comes from a crystal effect.

When the temperature rises above -20°C , thermal decomposition of the solution occurs, leading to the vanishing of the $\nu(\text{C}\equiv\text{O})$ signal at 1671 cm^{-1} whereas a band of medium-strong intensity rises at 1180 cm^{-1} , which can be due to $\nu(\text{P}=\text{O})$ of CH_3PO . No signal is detected for free CO_2 at 2340 cm^{-1} or for carbonyls between 1700 and 2000 cm^{-1} .

Normal Coordinate Analysis. There are no X-ray data on this complex, so structural parameters used to perform normal coordinate analysis were drawn from those of $\text{Cp}_2\text{Ti}(\text{CO})(\text{PMe}_3)$,⁶ replacing CO by CO_2 .

A complete calculation would be much too complicated because of the presence of the Cp ligands, for which no valence force field is available, those proposed by Cyvin¹¹ and Aleksanyan¹² being

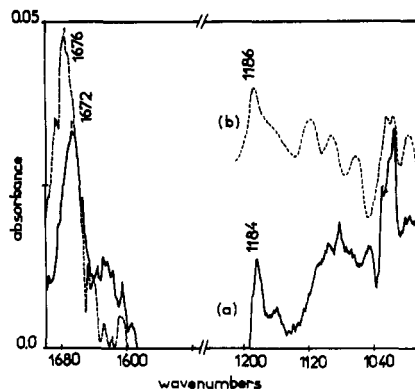


Figure 6. FTIR study of $\text{Cp}_2\text{Ti}(\text{CO}_2)(\text{PMe}_3)$ in solution in chloroform (a) and in dichloromethane (b) between 1700 and 950 cm^{-1} . (Solvents absorptions have been subtracted.)

not transferable in our case for symmetry reasons.

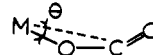
Furthermore, as we do not know the low-frequency absorptions, it is not necessary to run a complete calculation. So then each Cp ligand has been assumed to be a point mass Z of 65 g, with a force constant $f(\text{Ti}-Z)$ of 2 $\text{mdyn}\cdot\text{\AA}^{-1}$, as generally encountered in Cp_2M compounds with π bonding.¹³ As already done in part 1,¹ H atoms have been omitted for simplification in PMe_3 , the force field for PC_3 being that previously used for the *trans*- $\text{Mo}(\text{CO}_2)_2(\text{PMe}_3)_4$ and $\text{Fe}(\text{CO}_2)(\text{PMe}_3)_4$ complexes. Complete assignment of PMe_3 was published¹⁴ at the same time and confirmed our results.

The CO_2 moiety was initially side-on coordinated; geometric parameters and the valence force field for the $\text{Ti}(\text{CO}_2)$ unit were drawn from our previous study.¹

Then other coordination modes were envisaged, $\eta^1\text{-C}$ and $\eta^1\text{-O}$, for which structural parameters and valence force fields were transferred from our previous model studies in low-temperature matrices.⁴

In each case, the adjustment of the isotopic shifts had priority to that of frequencies themselves, as the former are more sensitive to the geometry of the molecule. Figure 7 gives the schematic representation of the geometry used to perform the normal coordinate analysis in the case of a $\eta^1\text{-C}$ coordination. The program used was the same as previously mentioned in part 1.¹

Table II compares the best final force fields obtained for each envisaged coordination mode. First of all, we can see that an out-of-the-plane bending mode $\gamma(\text{C}\equiv\text{O})$ cannot be defined in the case of an end-on coordination; it is replaced by a torsion motion $\tau(\text{CO})$ around the CO axis of $\text{M}-\text{O}-\text{C}\equiv\text{O}$ (that is why the order of magnitude of the force constant is completely different). But in this case, the isotopic frequency shift $^{16}\text{O}/^{18}\text{O}$ is enhanced and does not reproduce the observed values. A final comment relates to the possibility of a fluxional mechanism with interconversion $\eta^1\text{-O}$ and $\eta^2\text{-C,O}$ bonding modes such as shown as follows:



If $\theta = 0^\circ$ (end-on geometry), frequency shifts on $\tau(\text{CO})$ are respectively 7.5 and 18.5 cm^{-1} by $^{12}\text{C}/^{13}\text{C}$ and $^{16}\text{O}/^{18}\text{O}$ labeling. With opening of the angle θ to 21° (intermediate geometry), the frequency shifts are now equal (15 cm^{-1}). Finally, when $\theta = 38^\circ$ (side-on geometry), the frequency shift of $\gamma(\text{C}\equiv\text{O})$ for $^{12}\text{C}/^{13}\text{C}$ labeling is then more important (18 cm^{-1}) than that for $^{16}\text{O}/^{18}\text{O}$ enrichment (6 cm^{-1}), which is actually observed. We thus conclude that an end-on coordination does not seem likely in this complex.

If we compare now the frequency shifts expected by $^{16}\text{O}/^{18}\text{O}$ labeling on the $\nu(\text{CO})$ and $\delta(\text{C}=\text{O})$ modes for the $\eta^1\text{-C}$ and

(10) Demerseman, B.; Bouquet, G.; Bigorgne, M. *J. Organomet. Chem.* **1975**, *93*, 194.

(11) Brunvoll, J.; Cyvin, S. J. *J. Organomet. Chem.* **1971**, *27*, 107.

(12) Aleksanyan, V. T.; Vyshinskii, N. N.; Grinval'd, I. I.; Arsen'eva, T. I. *Bull. Acad. Sci. USSR* **1981**, *30*, 230.

(13) Nakamoto, K. In *Infrared and Raman Spectra of Inorganic and Coordination Compounds*; Wiley Interscience: New York, 1986.

(14) McKean, D. C.; McQuillan, G. P.; Murphy, W. F.; Zerbetto, F. *J. Phys. Chem.* **1990**, *94*, 4820.

Table II. Valence Force Fields for $\text{Cp}_2\text{Ti}(\text{CO})_2(\text{PMe}_3)$

modes ^a	Ti complex		
	end-on	side-on	C-coord
$\nu(\text{M-P})$	1.7	1.7	1.6
$\nu(\text{M-C})$		0.9	2.0
$\nu(\text{M-O})$	1.6	0.92	
$\nu_s(\text{PC}_3)$	2.62	2.62	2.62
$\nu'_s(\text{PC}_3)$	2.48	2.48	2.48
$\nu_a(\text{PC}_3)$	2.48	2.48	2.48
$\nu(\text{C-O})$	6.0	6.2	8.3
$\nu(\text{C=O})$	11.0	9.47	8.3
$\nu(\text{Ti-Z})^b$	1.0	1.0	1.98
$\delta(\text{CMO})$		0.25	
$\delta(\text{COM})$	0.35	0.35	
$\delta(\text{MCO})$		0.35	0.35
$\delta(\text{C=O})$	1.15	0.7	0.77
$\delta_s(\text{PC}_3)$	0.57	0.57	0.57
$\delta'_s(\text{PC}_3)$	0.64	0.64	0.64
$\delta_a(\text{PC}_3)$	0.64	0.64	0.64
$r_{\parallel}(\text{PC}_3)$	0.46	0.46	0.46
$r_{\perp}(\text{PC}_3)$	0.46	0.46	0.46
$\delta(\text{ZTiZ})$	0.1	0.1	0.2
$\delta(\text{PTiZ})$	0.1	0.1	0.2
$\delta(\text{CMP})$		0.28	0.28
$\delta(\text{OMP})$	0.28		
$\delta(\text{OTiZ})$	0.1	0.1	
$\delta(\text{CTiZ})$		0.1	0.2
$\gamma(\text{C=O})$	$\tau(\text{OC}) = 0.0051$	0.61	0.42
$\tau(\text{MC})$	$\tau(\text{MO}) = 0.0005$	0.0005	0.0005
$\tau(\text{MP})$	0.0005	0.0005	0.0005
$f[\nu(\text{C-O}), \nu(\text{C=O})]$	1.25	0.3	0.4
$f[\nu(\text{C-O}), \delta(\text{C=O})]$	-0.35	-0.1	0.0
$f[\delta(\text{TiOC}), \nu(\text{C-O})]$	0.4	0.0	
$f[\nu(\text{C=O}), \delta(\text{C=O})]$		0.0	0.0
$f[\nu(\text{C=O}), \delta(\text{MCO})]$		0.0	-0.1
$f[\nu(\text{C=O}), \nu(\text{MC})]$		0.0	0.4
$f[\delta(\text{C=O}), \delta(\text{MCO})]$		0.2	0.1
$f[\delta(\text{C=O}), \nu(\text{MC})]$		-0.4	0.0
$f[\delta_s(\text{PC}_3), \nu(\text{MP})]$	-0.15	-0.15	-0.15
$f[\delta(\text{C=O}), \nu_s(\text{PC}_3)]$		0.0	
$f[\delta(\text{C=O}), \delta(\text{MOC})]$	0.0		
$f[\delta(\text{C=O}), \nu(\text{MO})]$	0.0		

^a Force constants are given in $\text{mdyn}\cdot\text{\AA}^{-1}$ for bonds, $\text{mdyn}\cdot\text{\AA}^{-1}\cdot\text{rad}^{-2}$ for angles, and $\text{mdyn}\cdot\text{rad}^{-1}$ for bond-angle interactions. ^b Z = point mass for Cp.

$\eta^2\text{-C,O}$ bonding modes, we can see that, in the case of a true side-on coordination, this shift is larger for $\delta(\text{C=O})$ than for $\nu(\text{CO})$ (see results for *trans*- $\text{Mo}(\text{CO})_2(\text{PMe}_3)_4$ in part 1¹). For the titanium complex, like for $\text{Fe}(\text{CO})_2(\text{PMe}_3)_4$,¹ these effects are in the reverse order. So we could not fit the calculation with a side-on model, the best result giving respectively 26 cm^{-1} (vs 37 cm^{-1} observed) for the $\nu(\text{CO})$ shift and 33 cm^{-1} (vs 22 cm^{-1} observed) for the $\delta(\text{C=O})$ shift.

It then appeared that the titanium complex could have the same intermediate coordination between $\eta^1\text{-C}$ and $\eta^2\text{-C,O}$ as the iron compound previously studied.¹ But the fact that *no* $^{16}\text{O}/^{18}\text{O}$ isotopic shift has been observed below 500 cm^{-1} ruled out this hypothesis. In fact, the presence of a metal-oxygen bond would induce quite large oxygen frequency shifts in the 350–450- cm^{-1} region (9 cm^{-1} calculated on the mode at 427 cm^{-1}). See for example the results obtained in part 1,¹ where frequency shifts from 3 to 14 cm^{-1} were observed between 150 and 450 cm^{-1} for the molybdenum complex, whereas shifts from 4 up to 8 cm^{-1} occurred between 320 and 450 cm^{-1} for the iron compound.

So, the best fit between calculated and observed wavenumbers was obtained with a C-coordinated geometry.

Table III lists the results obtained and the assignments of the vibrational modes, along with calculated potential energy distribution. Good agreement is obtained between calculated and observed wavenumbers, showing that the final fitted force field with a C-coordinated bonding mode is relevant.

The CO bonds are equivalent with an intermediate character between a single and double bond: main force constants are 8.3

$\text{mdyn}\cdot\text{\AA}^{-1}$ with an interaction force constant equal to 0.4 $\text{mdyn}\cdot\text{\AA}^{-1}$. This last value indicates some amount of coupling, depending also on the value of the OCO valence bond angle, which is equal to 135° here.

So the out-of-phase stretching mode $\nu_{\text{op}}(\text{CO})$, observed at 1671 cm^{-1} , is calculated at 1674 cm^{-1} with isotopic shifts of 46 and 27 cm^{-1} for 42 and 23 cm^{-1} observed respectively by ^{13}C and ^{18}O labeling. The in-phase counterpart $\nu_{\text{p}}(\text{CO})$, observed at 1187 cm^{-1} , is calculated at 1193 cm^{-1} with frequency shifts of 23 and 32 cm^{-1} versus 32 and 37 cm^{-1} observed respectively by ^{13}C and ^{18}O enrichment.

The fit of $\Delta\bar{\nu}_{\text{p}}(\text{CO})$ by ^{13}C labeling is not so good, but none of the three models gave better results on this mode and we know from solution experiments that the value of 32 cm^{-1} is a maximum one because of the crystal effects. We must also keep in mind that the total amount of isotopic shifts observed on both modes is well reproduced (69 cm^{-1} calculated vs 74 cm^{-1} observed for $^{12}\text{C}/^{13}\text{C}$ isotopic effect and 59 cm^{-1} calculated vs 60 cm^{-1} observed for $^{16}\text{O}/^{18}\text{O}$ labeling). With comparison to previous matrix models⁴ (see also part 1), the relations $\bar{\nu}_3 - \bar{\nu}_1 \leq 400 \text{ cm}^{-1}$ and $\sum\Delta\bar{\nu}(^{13}\text{C}) \geq \sum\Delta\bar{\nu}(^{18}\text{O})$ with $60 < \sum\Delta\bar{\nu}(^{18}\text{O}) < 70 \text{ cm}^{-1}$ are quite well followed, as in this case we have $\bar{\nu}_3 - \bar{\nu}_1 = 484 \text{ cm}^{-1}$, $\sum\Delta\bar{\nu}(^{13}\text{C}) = 74 \text{ cm}^{-1}$, and $\sum\Delta\bar{\nu}(^{18}\text{O}) = 60 \text{ cm}^{-1}$. We can note that this $\eta^1\text{-C}$ geometry implies a mixing of the mode $\nu_{\text{p}}(\text{CO})$ with $\delta(\text{OCO})$ and $\nu(\text{TiC})$, for which resulting motion vectors are parallel. For example, the value of the interaction force constant $f[\nu(\text{CO}), \nu(\text{MC})]$ is the same as $f[\nu(\text{CO}), \nu(\text{CO})]$: 0.4 $\text{mdyn}\cdot\text{\AA}^{-1}$. The deformation $\delta(\text{OCO})$ is well reproduced, calculated at 722 cm^{-1} (observed at the same frequency) with isotopic shifts of 10 cm^{-1} (for 11 cm^{-1} observed) and 26 cm^{-1} (for 22 cm^{-1} observed), respectively, by ^{13}C and ^{18}O labeling. This mode is highly mixed with $\nu(\text{TiC})$ and $\nu_{\text{p}}(\text{CO})$, as indicated by the potential energy distribution. There is also a small coupling with $\nu'_s(\text{PC}_3)$, as indicated by small isotopic shifts on this mode. This coupling has not been introduced in the calculation, but the comparison of the total isotopic shifts gives now the following values: 10 cm^{-1} calculated vs 14 cm^{-1} observed by ^{13}C labeling and 26 cm^{-1} calculated vs 26 cm^{-1} observed by ^{18}O enrichment.

The out-of-the-plane motion $\gamma(\text{MOCO})$ is well-reproduced too, with a smaller force constant (0.42 $\text{mdyn}\cdot\text{\AA}\cdot\text{rad}^{-2}$) than in the side-on case (where average values are found between 0.6 and 0.7 $\text{mdyn}\cdot\text{\AA}\cdot\text{rad}^{-2}$). Finally, attribution of the absorptions at 427 and 393 cm^{-1} , respectively, to the $\nu_{\text{op}}(\text{TiCp})$ and $\nu(\text{TiP})$ vibrations fits well, the very weak absorption at 465 cm^{-1} remaining unassigned.

The main force constant for $\nu(\text{TiC})$ was initially evaluated as 2 $\text{mdyn}\cdot\text{\AA}^{-1}$ by comparison with previous results¹ (the sum of $f(\text{MO})$ and $f(\text{MC})$ in molybdenum and iron complexes is about 2 $\text{mdyn}\cdot\text{\AA}^{-1}$) and with values generally encountered for $f(\text{MC})$ in metal carbonyls.¹³ This value led to a calculated frequency for $\nu(\text{TiC})$ of 337 cm^{-1} . This mode is mixed with $\delta(\text{OCO})$ so that an isotopic shift of 8 cm^{-1} by ^{18}O labeling is expected. No refinement procedure could be done for lack of experimental data for this mode, but the calculated frequency is close to that found for $\text{Fe}(\text{CO})_2(\text{PMe}_3)_4$: 328 cm^{-1} with 4 cm^{-1} of $^{16}\text{O}/^{18}\text{O}$ isotopic shift because of mixing with the $\delta(\text{C=O})$ mode.¹

No important coupling between CO_2 and other ligands has been found in this compound.

Infrared Characterization of CO_2 Complexes. Table IV lists the final valence force fields obtained for the $\text{M}(\text{CO})_2$ unit in the three studied complexes $\text{Mo}(\text{CO})_2(\text{PMe}_3)_4$,¹ $\text{Fe}(\text{CO})_2(\text{PMe}_3)_4$,¹ and $\text{Cp}_2\text{Ti}(\text{CO})_2(\text{PMe}_3)$.

The metal- CO_2 vibrations are not easy to identify because they absorb at low frequency and have weak intensity and their isotopic shifts are small. Furthermore, they are often mixed with vibrations of coligands. For example, $\nu(\text{MoC})$ is mixed with $\delta(\text{PC}_3)$ in the molybdenum complex,¹ whereas $\nu(\text{FeO})$ and $\nu(\text{FeC})$ are highly mixed with all other vibrations of the equatorial plane in the iron compound.¹ For $\text{Cp}_2\text{Ti}(\text{CO})_2(\text{PMe}_3)$, the very weak intensity of the low-frequency region of the infrared spectra prevented us from observing the $\nu(\text{TiC})$ stretching mode. Anyway, we can see that, for the molybdenum complex, the force constants of MoO and MoC bonds are identical (0.9 $\text{mdyn}\cdot\text{\AA}^{-1}$) whereas, in the iron

Table III. Assignment of Observed and Calculated Wavenumbers (cm⁻¹) of Cp₂Ti(CO₂)(PMe₃) and Its Labeled Derivatives^a

Cp ₂ Ti(CO ₂)(PMe ₃)		Cp ₂ Ti(¹³ CO ₂)(PMe ₃)			Cp ₂ Ti(C ¹⁸ O ₂)(PMe ₃)			assgnts (PED)
obsd	calcd	obsd ^b		calcd ^c	obsd ^b		calcd ^c	
1671 (s)	1674	1629 (s)	42	46	1648 (s)	23	27	ν(CO) ₀₀ (100)
1285 (w)		1285 (w)			1286 (w)			δ _s (CH ₃)
1279 (w)		1280 (w)			1280 (w)			
1187 (m)	1193	1155 (w)	32	23	1150 (w)	37	32	ν(CO) ₀ (80), δ(OCO), ν(TiC)
1169 (m)		1167 (w)			1170 (sh)			crystal effect
1116 (m)		no			1099 (w)			oxygenated impurity
1075 (w)								
1070 (vw)		1073 (vw)			1073 (vw)			δ(CCC)
1062 (w)								
1025 (m)								
1019 (m)		1013 (m)			1016 (m)			δ(C-H)
1012 (m)								
961 (m)		961 (m)			961 (m)			r(CH ₃)
860 (sh)		863 (sh)			862 (sh)			γ(CH)
846 (sh)		846 (sh)			846 (sh)			
830 (sh)		830 (sh)			830 (sh)			r(CH ₃)
822 (sh)		822 (sh)			822 (sh)			
811 (s)		811 (s)			811 (s)			γ(CH)
741 (m)	741	738 (m)	3	0	737 (m)	4	0	ν _s (PC ₃) (96)
731 (m)	741	732 (m)	0	0	731 (m)	0	0	ν _a (PC ₃) (100)
722 (sh)	722	711 (sh)	11	10	700 (m)	22	26	δ(OCO) (38), ν(TiC) (25), ν(C-O) (17)
672 (sh)		672 (sh)			672 (sh)			crystal effect
668 (w)	662	668 (w)		0	668 (m)		0	ν _s (PC ₃) (92)
565 (w)	565	547 (w)	18	17	560 (w)	5	5.5	γ(MOCO) (100)
465 (vw)		no			no			?
427 (vw)	424	no		0.6	no		0.2	ν(TiCp) ₀₀
393 (w)	393	393 (vw)	0	0.1	392 (vw)	1	0.9	ν(TiP) (70), δ _s (PC ₃)

^ano = not observed; PED = potential energy distribution. ^bObserved frequency and difference values. ^cCalculated difference value.

Table IV. Comparison of Valence Force Fields for CO₂ Moieties in *trans*-Mo(CO₂)₂(PMe₃)₄, Fe(CO₂)(PMe₃)₄, and Cp₂Ti(CO₂)(PMe₃)^a

modes	Mo complex	Fe complex	Ti complex
ν(M-P)	1.6	MP _{ax} , 1.42 MP ₃ , 1.9 MP ₄ , 1.5	1.6
ν(M-C)	0.9	1.18	2.00
ν(M-O)	0.9	0.9	0
ν(C-O)	5.3	6.33	8.3
ν(C=O)	9.6	8.7	8.3
δ(CMO)	0.25	0.25	
δ(MOC)	0.35	0.35	
δ(MCO)	0.55	0.35	0.35
δ(C=O)	1.09	0.79	0.77
γ(C=O)	0.68	0.74	0.42
f[ν(C-O), ν(C=O)]	0	0.6	0.4
f[ν(C-O), δ(C=O)]	-0.4	0.13	0
f[ν(C-O), ν(M-C)]	-0.3	0	0
f[ν(C=O), δ(C=O)]	0	0.32	0
f[ν(C=O), δ(MCO)]	0	0	-0.1
f[ν(C=O), ν(M-C)]	0	0	0
f[δ(C=O), δ(MCO)]	0	0.2	0.1
f[δ(C=O), ν(M-C)]	-0.2	-0.4	0
f[δ(COM), δ(C=O)]	0	0.2	0

^aForce constants are given in m dyn·Å⁻¹ for bonds, m dyn·Å⁻¹·rad⁻² for angles, and m dyn·rad⁻¹ for bond-angle interactions.

compound, the force constant of FeC bonds is larger (1.2 m dyn·Å⁻¹) than the FeO one (0.9 m dyn·Å⁻¹). The sum of both force constants of the MO and MC bonds is approximately 2 m dyn·Å⁻¹, a value that can be compared to that evaluated for f(MC) in metal carbonyl complexes.¹³

Among the different compounds with carboxylic groups, it appears that the principal force constants for simple CO bonds vary from 4 to 6 m dyn·Å⁻¹ and from 9 to 15 m dyn·Å⁻¹ for double C=O bonds. That is what is observed for *trans*-Mo(CO₂)₂(PMe₃)₄,¹ where the difference f(C=O) - f(CO) is 4.3 m dyn·Å⁻¹. This splitting is less important for Fe(CO₂)(PMe₃)₄¹ (2.4 m dyn·Å⁻¹) and is zero in Cp₂Ti(CO₂)(PMe₃), where the two bands are equivalent and show an intermediate character between single and double bonds. This is also reflected by the interaction force constant f(C=O, CO), which is zero in the molybdenum complex

and positive for the other two complexes. This is an indication that the electronic delocalization is more important in the latter two and is related to the splitting of the two CO bonds stretching frequencies.

Among the other interaction force constants, we can see that f[ν(CO), δ(C=O)] and f[ν(CO), ν(MC)], negative for "true" side-on coordination, have positive values in other cases. As well, f[δ(C=O), ν(MC)], negative for molybdenum and iron complexes, is zero for the titanium compound. Ab initio calculations should lead to better understanding of electronic overlapping and interactions in these systems.

Finally, we can note that force constants for metallacycle vibrations



have arbitrary values. They have not been refined for lack of experimental data.

This article, along with previous ones,^{1,4} shows that it is possible to know the CO₂ bonding mode in organometallic complexes from very simple infrared spectroscopic observations.

First of all, it appears that study of labeled derivatives (¹³C and ¹⁸O) is necessary to fully assign the spectra.

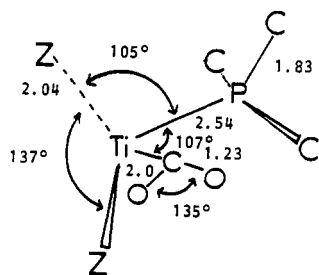
As soon as M(CO₂) vibrations are located by their frequency shifts, we can answer the following fundamental question: How is CO₂ linked to the metal in this compound?

The observation of a medium-intensity band around 500–600 cm⁻¹, with an important ¹²C/¹³C frequency shift (around 20 cm⁻¹) and a small one (around 5 cm⁻¹) by ¹⁶O/¹⁸O labeling, is the indication for a η¹-C or η²-C,O coordination. Then the splitting between the two CO stretching modes gives an additional indication. In fact, the amount of coupling will depend on the value of the OCO valence bond angle and on the difference between the two CO bonds force constants. The smaller is the difference, the larger is the coupling. Practically, a gap less than 400 cm⁻¹ must let one think that coordination is by the η¹-C mode. Other bonding modes give larger splittings (namely above 500 cm⁻¹).

Finally, the comparison of the sum of the isotopic shifts observed in the ν(C=O) and ν(CO) bands by ¹³C and ¹⁸O labeling will give additional signs for the CO₂ bonding mode. Side-on and η¹-C

Table V. Wavenumbers and Isotopic Shifts for ν_3 [$\nu(\text{C}=\text{O})$ or $\nu(\text{CO})_{\text{O}^{\oplus}}$] and ν_1 [$\nu(\text{CO})$ or $\nu(\text{CO})_{\text{C}^{\oplus}}$] Modes in Various CO_2 Complexes with Different Bonding Modes

complexes	$\bar{\nu}(\text{cm}^{-1})$	$\Delta\bar{\nu}^{(13\text{C})}$	Σ	$\Delta\bar{\nu}^{(18\text{O})}$	Σ	$\nu_3 - \nu_1$	structures
calcd values ⁴		47, 10	57	29, 52	81		end-on (C_s)
CuCO_2 (matrix) ⁴	1716, 1215	44, 10	54	29, 49	78	501	
OTiCO_2/Ar (matrix) ⁴	1730, 1185	45, 20	65	30, 50	80	545	
AlCO_2 (matrix) ¹⁶	1780, 1146	40, 19	59	39, 36	75	634	
calcd values ⁴		44, 21	65	23, 39	62		C-coord (C_{2v})
FeCO_2 (matrix) ⁴	1565, 1210	40, 25	65	25, 38	63	355	
$(\text{Pr-Salen})\text{Co}(\text{CO}_2)^-\text{K}^+$ ¹⁷	1650, 1280	40, 30	70			370	
	1215	23	63			435	
$\text{Cp}_2\text{Ti}(\text{CO}_2)(\text{PMe}_3)$	1671, 1187	42, 32	74	23, 37	60	484	
calcd values ⁴		40, 30	70	32, 20	52		side-on (C_s)
OTiCO_2 (matrix) ⁴	1735, 1132	33, 12?	45?	25, 32	57	603	
$\text{Mo}(\text{CO}_2)_2(\text{PMe}_3)_4$ ¹	1668, 1153	40, 29	69	30, 19	49	515	
	1102	26	66	26	56	566	
$\text{Fe}(\text{CO}_2)(\text{PMe}_3)_4$ ¹	1623, 1106	41, 16	57	29, 33	62	517	

**Figure 7.** Schematic representation of the geometry of the $\text{Cp}_2\text{Ti}(\text{CO}_2)(\text{PMe}_3)$ complex used to perform normal coordinate analysis with a $\eta^1\text{-C}$ bonding mode. (Bond lengths in Å.)

coordinations lead preponderant ^{13}C effects, whereas ^{18}O frequency shifts are very large for $\eta^1\text{-O}$ coordination.¹

But the influence of other ligands must be kept in mind, especially for the $\nu(\text{CO})$ and $\delta(\text{OCO})$ modes, which are often mixed together and/or are combined with coligand modes. Isotopic frequency shifts transfers can therefore occur and modify the balance of the isotopic shifts of several modes. This remark is especially true when vibrations of CO_2 and coligands, located in the same plane, are in close frequency. Isotopic shifts transfers are then the sign for coplanarity of CO_2 with a coligand in the whole molecule.

It also appears that study in solution is often necessary to fully understand the infrared solid-state spectra. Apart from crystal effects, CO_2 complexes are fluxional,¹⁵ and this property can afford special features in the spectra, as observed for *trans*- $\text{Mo}(\text{CO}_2)_2(\text{PMe}_3)_4$.¹

Table V lists the results obtained by us^{1,4} or other authors^{16,17} in low-temperature matrices and on organometallic species on the two CO stretching modes expected in CO_2 complexes. (Results obtained by Kafafi¹⁸ or Bencivenni¹⁹ on alkali metals have been omitted for clarity, but results obtained on MCO_2 complexes with end-on geometry fit well with our calculations.)

It appears that discrimination between the three bonding modes, end-on (symmetry C_s), side-on (C_s), and C coordination (C_{2v}), by measurement of isotopic shifts observed on the two $\nu(\text{CO})$ stretching modes (ν_1 , ν_3) is possible. Observations of these values and the splitting ($\nu_3 - \nu_1$) are good criteria for unequivocal characterization of $L_n\text{MCO}_2$ complexes.

Anyway, this work must be completed by infrared study of other CO_2 complexes for which the X-ray structures are known, such as the $\eta^1\text{-C}$ complex $(\text{pr-Salen})\text{Co}(\text{CO}_2)^-\text{K}^+$ ¹⁷ and the side-on one $\text{Cp}_2\text{Mo}(\text{CO}_2)$.²⁰

Conclusions

The experiments described in our two papers have shown how isotopic labeling in FTIR techniques along with normal coordinate treatment can afford unequivocal characterization of CO_2 -metal bonding modes in organometallic complexes.

Complete assignments and calculation of valence force fields have been made for the three studied compounds. The main conclusions are (i) CO_2 is side-on coordinated in *trans*- $\text{Mo}(\text{CO}_2)_2(\text{PMe}_3)_4$, the coupling between the two CO_2 vibrations resulting from fluxionality of the CO_2 moieties, (ii) the strong Fe-C bond and coupling of coplanar phosphorous ligands with CO_2 encountered in $\text{Fe}(\text{CO}_2)(\text{PMe}_3)_4$ implies an intermediate coordination mode between $\eta^1\text{-C}$ and $\eta^2\text{-C,O}$ bonding, and, (iii) in $\text{Cp}_2\text{Ti}(\text{CO}_2)(\text{PMe}_3)$, CO_2 is C-coordinated to the metal.

In addition, our experiments have introduced new experimental approaches of infrared analysis for such compounds: (i) We have confirmed that $\nu(\text{C}=\text{O})$ bands (1800–1600 cm^{-1}) do not discriminate significantly between CO_2 complexes and other carboxylic compounds. (ii) We have shown the importance, besides ^{13}C labeling, of ^{18}O enrichment in the infrared study. For example, the mode $\delta(\text{C}=\text{O})$ is very sensitive to the electronic effects of coligands and the frequency shift obtained by ^{18}O labeling is a good indicator of the CO_2 moiety localization in the complex. As well, isotopic shifts of $\nu(\text{CO})$ and $\gamma(\text{C}=\text{O})$ frequencies are directly related to the metal- CO_2 bonding mode.

It also appears that several spectroscopic techniques (FTIR, NMR) must be focused onto a single dynamic problem. When these techniques are combined with synthetic chemistry, significant new insights can be obtained, even into previously well-known complexes.

For example, the ^{13}C -labeled derivatives obtained for infrared purposes can be used to measure the coupling between CO_2 and phosphorus in these compounds by ^{13}C NMR spectroscopy and to obtain additional structural conclusions. Furthermore, the mechanisms of fluxionality predicted by theory and observed, for example, in *trans*- $\text{Mo}(\text{CO}_2)_2(\text{PMe}_3)_4$ ²¹ and $\text{Ni}(\text{CO}_2)(\text{PCy}_3)_2$,²² must be studied by both spectroscopies, as the time scales are different and allow one to observe fast and slow motions. This implies a better understanding of temperature-dependent infrared spectra for such complexes in solution.

Equally, our experiments have underlined the unexpected role of FTIR analysis in the characterization of such complexes. Such analysis in solution media should lead to the discovery of new intermediates in catalytic reduction processes of CO_2 .

Acknowledgment. We thank Prof. H. G. Alt, C. Biran, and E. Samuel for their assistance in the synthesis of $\text{Cp}_2\text{Ti}(\text{CO}_2)(\text{PMe}_3)$. Finally, we thank B. Janocha, an undergraduate student from the University of Mainz (FRG), who has contributed to this project through his project work (Oct 1989–July 1990).

- (15) Mealli, C.; Hoffmann, R.; Stockis, A. *Inorg. Chem.* **1984**, *23*, 56.
 (16) Le Quere, A. M.; Xu, C.; Manceron, L. *J. Phys. Chem.*, in press.
 (17) Fachinetti, G.; Floriani, C.; Zanazzi, P. F. *J. Am. Chem. Soc.* **1978**, *100*, 7405.
 (18) Kafafi, Z. H.; Hauge, R. H.; Billups, W. E.; Margrave, J. L. *J. Am. Chem. Soc.* **1983**, *105*, 3886.
 (19) Teghil, R.; Janis, B.; Bencivenni, L. *Inorg. Chim. Acta* **1984**, *88*, 115.
 (20) Gambarotta, S.; Floriani, C.; Chiesi-Villa, A.; Guastini, G. *J. Am. Chem. Soc.* **1985**, *107*, 2985.

- (21) Carmona, E.; Munoz, M. A.; Perez, P. J.; Poveda, M. L. *Organometallics* **1990**, *9*, 1337.
 (22) Aresta, M.; Quaranta, E.; Tommasi, I. *J. Chem. Soc., Chem. Commun.* **1988**, 450.